$N=14$ and 16 shell gaps in neutron-rich oxygen isotopes

M. Stanoiu,[1,2] F. Azaiez,[2] Zs. Dombrádi,[3] O. Sorlin,[2] B. A. Brown,[4] M. Belleguic,[2] D. Sohler,[3] M. G. Saint Laurent,[1] M. J. Lopez-Jimenez,[1] Y. E. Penionzhkevich,[5] G. Sletten,[14] N. L. Achouri,[6] J. C. Angélique,[6] F. Becker,[1] C. Borcea,[7] C. Bourgeois,[2] A. Bracco,[8] J. M. Daugas,[1] Z. Dlouhý,[9] C. Donzaud,[2] J. Duprat,[2] Zs. Fülöp,[3] D. Guillemaud-Mueller,[2] S. Grévy,[6] F. Ibrahim,[2] A. Kerek,[10] A. Krasznahorkay,[3] M. Lewitowicz,[1] S. Leenhardt,[2] S. Lukyanov,[5] P. Mayet,[11] S. Mandal,[11] H. van der Marel,[10] W. Mittig,[1] J. Mrázek,[11] F. Negoita,[7] F. De Oliveira-Santos,[1] Zs. Podolyák,[12] F. Pougheon,[2] M. G. Porquet,[13] P. Roussel-Chomaz,[1] H. Savajols,[1] Y. Sobolev,[5] C. Stodel,[1] J. Timár,[3] and A. Yamamoto[12]

[1]*GANIL BP 55027,14076 Caen Cedex 5, France*

[2]*IPN, IN2P3-CNRS and Université Paris-Sud, F-91406 Orsay Cedex, France*

[3]*Institute of Nuclear Research, P.O. Box 51, H-4001 Debrecen, Hungary*

[4]*NSCL, East Lansing, Michigan 48824-1321, USA*

[5]*FLNR, JINR, 141980 Dubna, Moscow region, Russia*

[6]*LPC, IN2P3-CNRS, ISMRA et Université de Caen, F-14050 Caen Cedex, France*

[7]*IFIN-HH PO-BOX MG-6, 76900 Bucharest Magurele, Romania*

[8]*Dipartimento di Fisica, Universita' di Milano and INFN sezione di Milano, Italy*

[9]*Nuclear Physics Institute, 25068 Řež, Czech Republic*

[10]*Royal Institute of Technology, Alba Nova University Center, S-106 91 Stockholm, Sweden*

[11]*GSI Postfach 110552, D-64220 Darmstadt, Germany*

[12]*Department of Physics, University of Surrey, Guildford, GU2 5XH, United Kingdom*

[13]*CSNSM, IN2P3-CNRS and Université Paris-Sud, F-91405 Orsay Cedex, France*

[14]*The Niels Bohr Institute, Blegdamsvej 17, DK-2100, Copenhagen, Denmark*

(Received 23 September 2003; published 10 March 2004)

In-beam γ-ray spectroscopy using fragmentation reactions of both stable and radioactive beams has been performed in order to study the structure of excited states in neutron-rich oxygen isotopes with masses ranging from $A=20$ to 24. For the produced fragments, γ-ray energies, intensities, and γ-γ coincidences have been measured. Based on this information new level schemes are proposed for ^{21,22}O up to the neutron separation energy. The nonobservation of any γ-decay branch from ^{23}O and ^{24}O suggests that their excited states lie above the neutron decay thresholds. From this, as well as from the level schemes proposed for ^{21}O and ^{22}O, the size of the $N=14$ and 16 shell gaps in oxygen isotopes is discussed in the light of shell-model calculations.

DOI: 10.1103/PhysRevC.69.034312 PACS number(s): 23.20.Lv, 21.60.Cs, 27.20.+n, 27.30.+t

I. INTRODUCTION

The structure of atomic nuclei is known to be largely dominated by the single-particle shell effects. For instance, basic nuclear properties such as binding energies and shapes depend strongly on the underlying shell structure. The study of nuclei beyond the valley of stability helps one to understand the way single-particle energies evolve when one goes away from stable nuclei to the neutron and proton drip lines. Such evolutionary studies facilitate more precise predictions of the limit of existence of nuclear species. In the case of light nuclei, the rapid change in the location of the neutron drip line between the O and F isotopes is still not understood. The neutron drip line seems to be reached at $N=16$ in O isotopes whereas in the neighboring F isotopes, it has been found to extend up to $N=22$ [1,2]. Obviously, the understanding of how shell structure evolves when going from oxygen to fluorine nuclei would shed light on how the nuclear force can facilitate the binding of six neutrons by the addition of a single proton as in ^{31}F.

Excited states in the neutron-rich O isotopes were previously reported by Catford *et al.* [3] using transfer reactions. The first excited 2^+ state of the $N=14$ nucleus ^{22}O is 3190 keV [4,5]. This is almost two times higher than in the adjacent $N=10$ and 12 nuclei and therefore indicates the presence of a $N=14$ (sub)shell closure. This finding is also supported by the $B(E2)$ value deduced from the inelastic scattering experiments of Ref. [5]. While the systematics of the first excited 2^+ in neon isotopes show the disappearance of the $N=20$ shell closure, a new shell effect at $N=16$ seems to appear [4]. This new $N=16$ gap in the *sd*-shell nuclei is also substantiated by neutron separation energies deduced from mass measurements [6,7].

Experimental studies using interaction cross-section measurements [8] and longitudinal momentum ($P_{\|}$) distributions after one-and two-neutron removal [10] are consistent on a halo structure in ^{23}O, although it was shown in Ref. [9] that the one- and two-neutron removal data could be understood in the *sd*-shell model without the need for a halo. In Ref. [8] a lowering of the *s* orbital was suggested as giving rise to the $N=16$ magic number in the heaviest oxygen isotopes.

In this paper we shall report on experiments probing the structure of $N=12-16$ oxygen isotopes by way of fragmentation reactions and γ-ray spectroscopy. The experimental technique is described in Sec. II and the results and their interpretation follow in Sec. III.

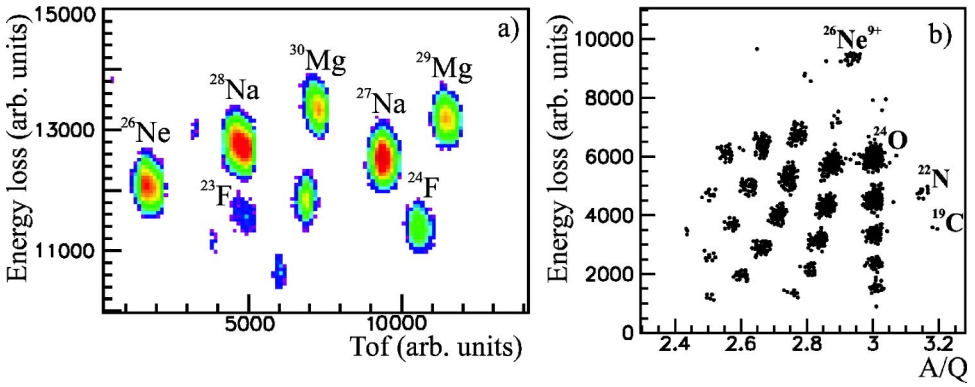

FIG. 1. (Color online) (a) Secondary beam composition given by the time of flight and energy loss information from the "active" target. (b) Energy loss vs mass over charge identification spectrum of the fragments produced in the active target and selected through the SPEG spectrometer.

II. EXPERIMENTAL TECHNIQUES

In order to obtain information on the structure of neutron-rich nuclei in the proton *sd*-shell region, in-beam γ-ray spectroscopy using projectile fragmentation reactions has been performed. Two experiments using the fragmentation of a stable ^{36}S beam have been done at GANIL. Both experiments are based on coincidence measurements between the projectilelike fragments and their prompt γ decay. A common γ-detector array has been used in both experiments. It consists of 74 BaF_2 detectors placed at a mean distance of 30 cm from the target and covering nearly 4π. The relatively high velocity of the produced projectile fragments ($v/c \simeq 0.35$) necessitates a proper Doppler correction of the detected γ-rays energies. The total photo-peak efficiency of the BaF_2 array was found to be 30% at 1.3 MeV with an average full width at half maximum of 12% after Doppler correction. The energy threshold of the BaF_2 detectors has been adjusted to a minimum value in order to allow the detection of low-energy γ rays down to 100 keV. The produced fragments were selected and identified in the SPEG spectrometer by the use of time of flight, energy loss, and focal-plane position information.

In the first experiment a 77.5 MeV A ^{36}S beam with an intensity of about 1 pnA was fragmented on a thin Be foil (2.77 mg/cm^2) located at the target place of SPEG, the energy loss spectrometer at GANIL. The SPEG was tuned to the $A/Z=2.75$ mass to charge ratio, that is between ^{21}O and ^{22}O. As a result, the nuclei ^{20,21,22,23}O were transmitted. During the experiment we observed 7500 ^{23}O, 426×10^3 ^{22}O, 1.7×10^6 ^{21}O, and 230×10^3 ^{20}O nuclei. In addition to the BaF_2 array, four 70% high resolution Ge detectors were used at the most backward angles. The overall Ge detector efficiency was 0.12% at 1.3 MeV. In spite of having a low efficiency, the high resolution of the Ge detectors ($\sim$30 keV at 1.3 MeV after Doppler correction) helped to disentangle complex spectra just as those obtained for ^{21}O. The BaF_2 array coincidence efficiency exceeded the Ge efficiency by 1-2 orders of magnitude, especially at high energies. By gating on high-energy transitions (in the BaF_2) sitting on low background one could identify transitions not seen in the Ge spectra. A few transitions in ^{22}O could be observed only in this way. Henceforth we shall refer to this measurement as a "single step fragmentation" (SSF) experiment.

In the second experiment, we used a primary beam of ^{36}S delivered by the two GANIL cyclotrons at an energy of 77.5 MeV A and an intensity of 400 pnA on a carbon target of 348 mg/cm^2 thickness placed in the SISSI spectrometer. The produced nuclei were selected through the ALPHA spectrometer using a 130 mg/cm^2 Al wedge. The magnetic rigidity of the ALPHA spectrometer and the optics of the beam line were optimized for the transmission of a cocktail beam mainly composed of ^{24}F, ^{25,26}Ne, ^{27,28}Na, and ^{29,30}Mg fragments with energies varying from 54 MeV A to 65 MeV A [see Fig. 1(a)]. An "active" target composed of a plastic scintillator (103 mg/cm^2) sandwiched by two carbon foils of 51 mg/cm^2 thickness was used at the same place as the Be target in the SSF experiment. The plastic scintillator portion of this active target was used on an event by event basis to identify the incoming nuclei via their energy loss and time of flight [see Fig. 1(a)]. The fragments produced by reactions of the secondary beam in the active target are selected and identified at the SPEG focal plane which was optimized for ^{24}O acceptance ($A/Z=3$). As shown in Fig. 1(b), neutron-rich nuclei with Z ranging from 4 to 10 were also measured. This method, which has also been applied at RIKEN [11], is called "double step fragmentation" (DSF) method because it uses two consecutive fragmentation reactions for the production of the nuclei of interest.

Noteworthy is the fact that in the case of SSF the ^{36}S beam intensity was limited to 6×10^9 pps in order to keep the singles rate in the individual γ-ray detectors $\leqslant 2\times10^4$ s^{-1}. This is a critical limitation for this method, as the production cross sections of interest are of the order of ~1 μb, or $\sim10^{-6}$ of the total cross section. As a consequence, the γ-ray spectroscopy of ^{24}O was beyond reach in the first experiment.

In the case of DSF a secondary cocktail beam comprised of nuclear species similar to the nuclei of interest was used with an intensity of only 8×10^4 s^{-1}. Given such a low secondary beam intensity, only γ-ray spectroscopy of those exotic nuclei produced with relatively high ($\sim$0.1 mb) cross sections was possible. Nevertheless, ^{24}O was produced with almost a factor 10 higher intensity than it could have been produced with the SSF technique. Another issue that must be taken into account is the γ-ray peak/background ratio. In the case of the SSF method, some of the nuclei of interest are populated through a reaction where more than one nucleus is excited. This is an additional source of background as γ rays from all these nuclei are emitted in coincidence and only those emitted from the fragments that are having the proper velocity, show up as discrete lines in the Doppler corrected

γ-ray spectrum. In the case of the DSF method, the nuclei of interest are produced via reactions involving the removal of only a few nucleons, which reduces the sources of background to the γ rays emitted from the quasiprojectile nuclei. Another equally important contribution to the background comes from neutron emission. DSF is less susceptible to this type of background in the measured γ-ray spectra, as in this case the process is cooler and so, a smaller number of neutrons are produced as compared to SSF. Moreover, the raw counting rates of individual γ-ray detectors were reduced by two orders of magnitude compared to the SSF experiment.

III. EXPERIMENTAL RESULTS AND DISCUSSIONS

Most of the results that will be presented in this section are interpreted in the light of shell-model calculations. These calculations are based upon the full *sd* shell for $A=16$ nucleons outside of a closed core of ^{16}O. We use the Universal *sd*-shell (USD) hamiltonian [12,13] which consists of three single-particle energies for $d_{5/2}$, $s_{1/2}$, and $d_{3/2}$ and 63 two-body matrix elements (TBME)—only the 30 matrix elements with $T=1$ are needed for neutron configurations of the oxygen isotopes. The USD single-particle energies are close to those observed in ^{17}O. The USD interaction is a set of TBME which were obtained from a least-squares fit of 47 linear combinations of TBME to 447 binding energy data in the mass region $A=16-40$ as they were known up to 1983. The starting set of TBME was based on the Kuo-Brown renormalized *G* matrix [14], and the 16 remaining linear combinations of TBME were kept at their *G* matrix values. The USD energy levels for all of the *sd*-shell nuclei are given in Ref. [16]. (The levels in this database labeled by an asterisk are those used for the least-squares fit.) Of particular importance for this work are the constraints placed on the $T=1$ matrix elements by the oxygen data as they were known up to about the year 1983—the three single-particle states in ^{17}O, the ground state binding energies of $^{18-21}$O, the excitation energy of the 2^+, 4^+, and 3^+ states in ^{18}O, seven excited states in ^{19}O, and three excited states in ^{20}O (these are the states labeled by asterisk in Ref. [16]). The results we discuss for $^{21-24}$O are predictions of this USD interaction.

In order to understand the results it is useful to define the effective single-particle energies (ESPE) for the three neutron orbits. These are the bare single-particle energies (those in ^{17}O) plus the addition of the monopole part of the diagonal TBME with the assumption of closed-shell configurations for ^{22}O and ^{24}O. The monopole interaction contribution is the $(2J+1)$ weighted average of the diagonal TBME multiplied by the $n(n-1)/2$ for the self-interaction in a single orbit or n_1n_2 for the interaction between two orbits (n is the orbit occupancy). The ESPE for the oxygen isotopes with the USD interaction is shown in Fig. 16 of Ref. [17]. The $d_{5/2}-s_{1/2}$ gap starts out at 0.8 MeV for ^{16}O and increases to 4.3 MeV in ^{22}O ($N=14$). This gap is large enough to make ^{22}O a magic nucleus (e.g., the shell gap is much larger than the pairing gap). In addition at $N=16$ there is a 4.5 MeV gap between the $s_{1/2}$ and $d_{3/2}$ orbits which also makes ^{24}O a magic nucleus. In terms of the present data on energy levels, the signature of a magic nucleus is an energy of the first 2^+ state, which is significantly higher than the neighboring even-even nuclei.

If one assumes a closed-shell $(0p-0h)$ model for ^{22}O, the $s_{1/2}$ $(1p)$ ESPE is given by the energy difference between the ^{23}O and ^{22}O ground states energies [$\tilde{\epsilon}(s_{1/2})=-2.74(12)$ MeV from experiment], and the $d_{5/2}$ $(1h)$ ESPE is given by the ^{22}O$-^{21}$O energy difference [$\tilde{\epsilon}(d_{5/2})=-6.85(6)$ MeV from experiment]. Thus from the experimental ground state binding energies one would estimate $\tilde{\epsilon}(s_{1/2})-\tilde{\epsilon}(d_{5/2})=4.11(13)$ MeV for the gap. The USD values obtained with a closed-shell configuration are $\tilde{\epsilon}(s_{1/2})=-2.47$ MeV, $\tilde{\epsilon}(d_{5/2})=-6.79$ MeV, and $\tilde{\epsilon}(s_{1/2})-\tilde{\epsilon}(d_{5/2})=4.32$ MeV (the value given above). In the full *sd*-shell calculation with USD one gets $\tilde{\epsilon}(s_{1/2})=-2.45$ MeV, $\tilde{\epsilon}(d_{5/2})=-7.15$ MeV and $\tilde{\epsilon}(s_{1/2})-\tilde{\epsilon}(d_{5/2})=4.70$ MeV.

The large $d_{5/2}-s_{1/2}$ gap at $N=14$ is an essential new feature of the USD interaction, which is different from what one gets with the *G* matrix. The *ab initio* calculations based upon the renormalized *G* matrix have an ESPE $d_{5/2}-s_{1/2}$ gap at $N=14$ which is only 0.9 MeV, and ^{22}O is not a magic nucleus. With the *G*-matrix hamiltonian the ground state of ^{22}O is 29% $0p-0h$, 61% $2p-2h$, 3% $3p-3h$, and 7% $4p-4h$, and the 2^+ energy is 1.71 MeV. Energies of excited states in $^{18-20}$O which have a large component with one neutron in the $s_{1/2}$ orbit were important in the determination of the USD matrix elements which are essential for the theoretical extrapolations to $^{21-23}$O [20]. The two diagonal matrix elements $\langle(d_{5/2},s_{1/2});J,T=1|V|(d_{5/2},s_{1/2});J,T=1\rangle$ with $J=2$ and 3 are the most important. This is an example of how the nuclear shell model with effective two-body matrix elements can be used to relate data on excited states in nuclei near stability to the properties of more exotic nuclei—in this case out to the neutron drip line.

A. The oxygen isotope $A=20$

As mentioned earlier the energies of the excited states in this isotope have been used as input to the shell-model calculations. The data on this isotope have been obtained only from the SSF experiment. γ rays from high-lying excited states of ^{20}O are observed. The γ-ray spectrum measured in the Ge detectors is shown in Fig. 2. All the observed transitions fit well into the level scheme from earlier multinucleon transfer reactions [15] as it can be seen in Fig. 3. Their placement is supported also by the coincidence relationship observed in our data using the BaF_2 detectors. Some of the previously known states are missing in our case, probably due to a different feeding pattern of the excited states.

Relative to a $0p-0h$ configuration for ^{22}O, the lowest states in ^{20}O are those expected from the $0p-2h$ configuration with the two holes in $d_{5/2}$ coupled to $J=0$, 2, and 4. The higher states in ^{20}O are dominated by $1p-3h$ with the one particle in $s_{1/2}$ and the three holes in $d_{5/2}$ coupled to $J=3/2$, $5/2$, and $7/2$.

B. The oxygen isotope $A=21$

The ^{21}O isotope has been produced with relatively high statistics in both SSF and DSF experiments. The γ-ray spec-

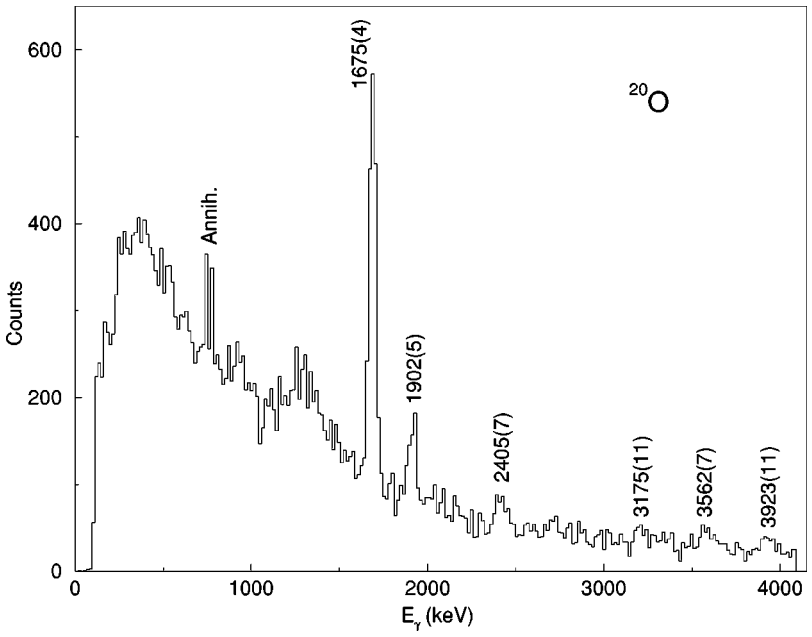

FIG. 2. γ-ray spectrum of ^{20}O obtained from Ge detectors in the SSF experiment. The doublet of sharp lines at about 730 keV and marked as Annih represents the 511 keV annihilation γ-ray radiation after Doppler correction to account for the velocity of the emitting fragments and for the two different angles of the Ge detectors.

trum obtained in the Ge detectors is shown in Fig. 4. This nucleus has been studied earlier by transfer reactions [3] and the existence of four excited states has been revealed. The spin and parity of the ground state has been recently suggested by Sauvan *et al.* [19] to be $5/2^+$.

Based on γ-ray coincidences from the BaF_2 detectors, we have built a level scheme of ^{21}O. The level scheme is compared in Fig. 5 to the previous work of Catford *et al.* [3] and to shell-model calculations [16].

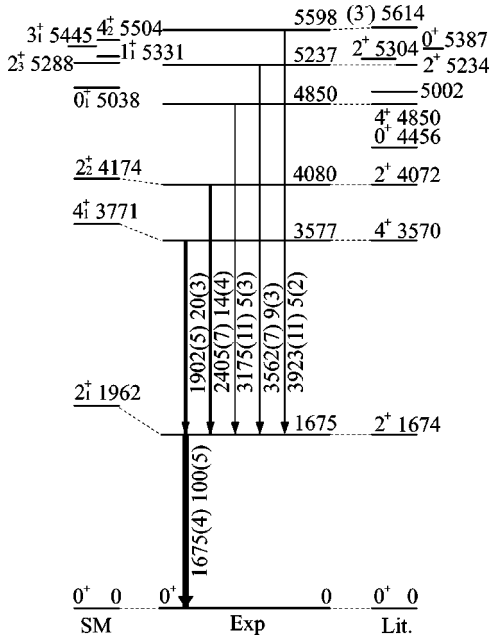

FIG. 3. The ^{20}O level scheme obtained from the present work, the USD shell-model calculations and from transfer reactions. Tentative associations between observed and calculated levels are indicated by dashed lines. Transition energies and relative intensities are indicated together with their uncertainties for the experimental work.

As can be seen in Fig. 5, a very good agreement is found between the proposed level scheme and the one calculated within the USD shell model [17]. It is also remarkable that the level scheme reported by Catford *et al.* [3] from inclusive multinucleon transfer reactions performed more than ten years ago is in agreement with our level scheme extracted from γ-γ coincidence technique. As an example, Fig. 6 shows the coincidence relationship between γ-ray transitions used in the level scheme. It is interesting to note that the highest energy state observed in the fragmentation reactions is about 1 MeV higher than the neutron separation energy (S_n=3.807 MeV). To prove the existence of this state, we show the coincidence relation observed between the 1.854 and 3.07 MeV transition in Fig. 6.

Relative to the dominant closed $d_{5/2}$ shell for ^{22}O ground state which will be called $0p-0h$, the structure of ^{21}O can be interpreted in terms of the $0p$-$1h$ $5/2^+$ ground state and the $1p$-$2h$ excited states based upon coupling of the $s_{1/2}$ (particle) orbit to the $(d_{5/2})^{-2}$ $2h$ states (0^+, 2^+ and 4^+) to give the ^{21}O excited states $1/2^+$, $(3/2^+, 5/2^+_2)$ and $(7/2^+, 9/2^+)$, respectively. This accounts for all of the shell-model levels (in the full-space calculation) up to 4.7 MeV and all of the levels observed in this experiment. The excitation energies of these states are determined by the $d_{5/2}$-$s_{1/2}$ single-particle gap, the $2h$ interaction energy and the $1p$-$2h$ interaction energy (e.g., the part related to the $1p$-$1h$ splitting in ^{22}O). The spacing of the $2h$ states is related to the low-lying state of ^{20}O, 0^+ (g.s.), 2^+ (1.64 MeV) and 4^+ (3.57 MeV).

In the full *sd*-shell USD model, the centroid energy of the $(7/2^+, 9/2^+)$ doublet relative to the $5/2^+$ ground state of 4.0 MeV is close to the $d_{5/2}$-$s_{1/2}$ ESPE gap of 4.3 MeV. Thus the experimental spacing of 4.1 MeV for $(7/2^+, 9/2^+)$-$5/2^+$ is a good measure of the the $d_{5/2}$-$s_{1/2}$ ESPE energy gap. The spacing $1/2^+$-$5/2^+$ is only 1.22 MeV (2.7 MeV lower than the ESPE) due to the pairing interaction in the $2h$ 0^+ configuration.

The predicted γ-decay properties of $^{20-22}$O are given in Ref. [16]. In the simplest model the states in the $1p$-$2h$ dou-

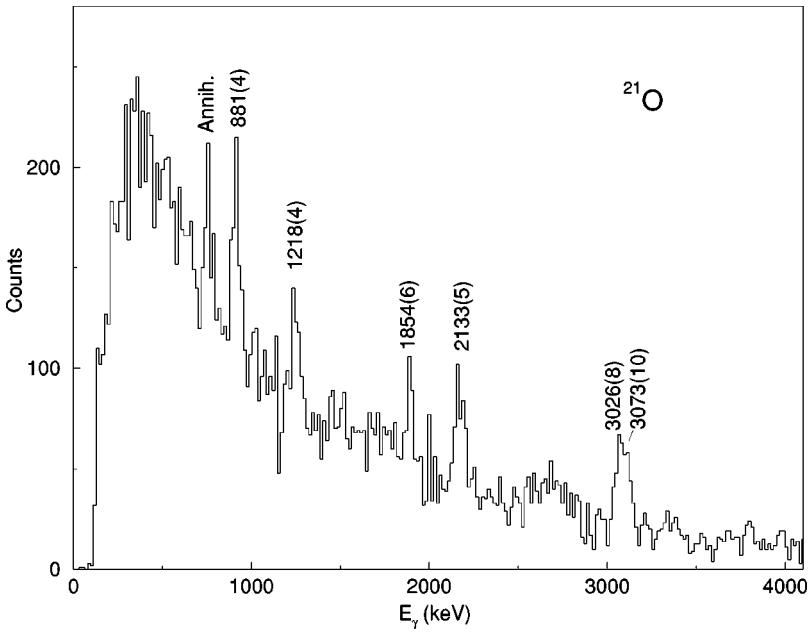

FIG. 4. γ-ray spectrum of ^{21}O obtained from the Ge detectors in the SSF experiment "Annih." indicates the annihilation radiation line after Doppler correction.

blets can all decay to the $1h$ ground state by $E2$. This can be seen by recoupling $1p$-$2h$ into $[(1p-1h)J_c \times 1h]$ where the hole is in $d_{5/2}$. Thus, up to some recoupling factors the $E2$ strength is proportional to the $0p-0h(0^+) \rightarrow 1p-1h(2^+)$ strength in ^{22}O. Transitions between the $1p-2h$ doublets can only go by the $E2$ transitions between the $2h$ components (given in parentheses); $3/2^+ \rightarrow 1/2^+(2^+ \rightarrow 0^+)$, $5/2_2^+ \rightarrow 1/2^+(2^+ \rightarrow 0^+)$, $7/2^+ \rightarrow 3/2^+(4^+ \rightarrow 2^+)$, $9/2^+ \rightarrow 5/2_2^+(4^+ \rightarrow 2^+)$, and $9/2^+ \rightarrow 3/2^+(4^+ \rightarrow 2^+)$. In addition, there are transitions between the members for the doublets $5/2_2^+ \rightarrow 3/2^+$ and $9/2^+ \rightarrow 7/2^+$ which are dominantly $M1$. In the full space calculations the strong $M1$ between the members of the doublet are quenched and the forbidden $M1$ are allowed. Thus all possible $M1$'s become moderate in strength and all decays are dominated by the $M1$ component when allowed. The experimental decay scheme is in good overall agreement with the calculations.

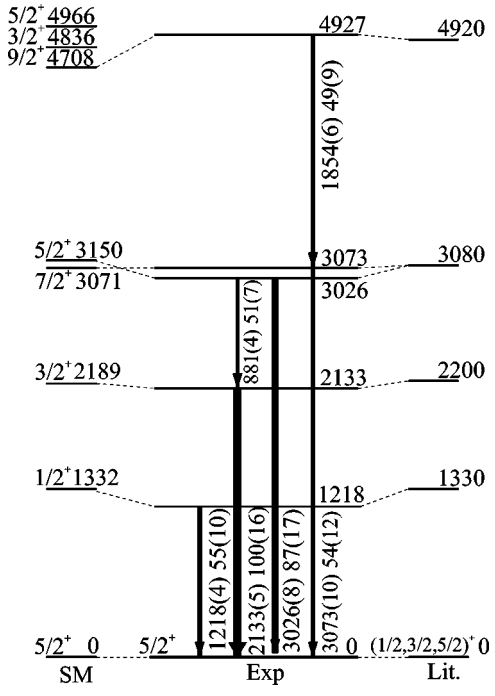

FIG. 5. Energy diagram for ^{21}O from the present work with USD shell-model calculations and transfer reactions. Tentative associations between observed and calculated levels are indicated by dashed lines. Transition energies and relative intensities are indicated together with their uncertainties for the experimental work.

The decay of the $9/2^+$ state, which was already observed

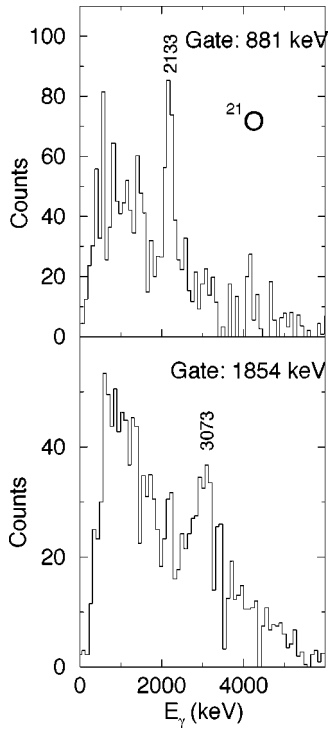

FIG. 6. γ-γ coincidences observed in ^{21}O using the BaF_2 array in the SSF experiment.

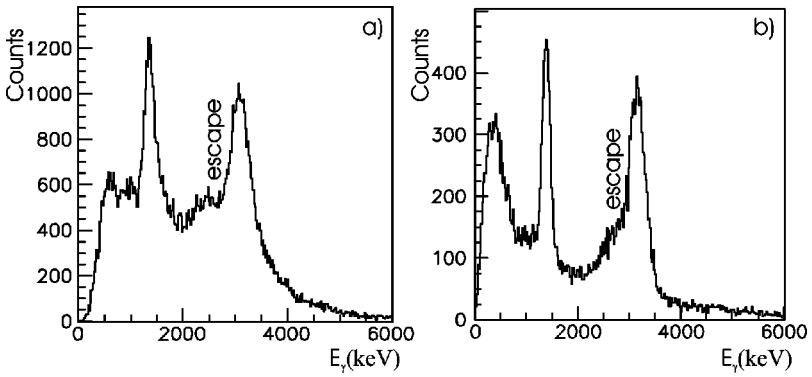

FIG. 7. γ-ray spectrum of ^{22}O. (a) Obtained from the BaF_2 detectors in the SSF experiment. (b) The same spectrum obtained during the DSF measurement. In both BaF_2 spectra of (a) and (b), the single escape line of the 3.15 MeV γ transition is indicated by "escape." Note the lower energy threshold used for the BaF_2 detectors in the DSF experiment

by Catford *et al.* [3] as a narrow resonance in their transfer reaction, is interesting. It is unbound by 1.1 MeV to an $\ell=4$ neutron emission to the ^{20}O ground state. Nevertheless it is observed to γ decay. In the *sd* shell this $\ell=4$ transition is forbidden, and the γ decay puts a limit on the spectroscopic factor which may arise from mixing from the sdg major shell. In the USD calculation the γ decay is dominated (75%) by a moderately strong $M1$ between the two members of the ($7/2^+$, $9/2^+$) doublet (the weaker 25% decay to the $5/2^+$ ground state would not have been observed in this experiment). The calculated lifetime is 57 fs. The single-particle width for an $\ell=4$ decay obtained from a typical Woods-Saxon potential is 0.31 keV or a lifetime of 0.0020 fs. Thus the spectroscopic factor for the $\ell=4$ decay of the $9/2^+$ state must be less than 0.029. We have used a much larger $2\hbar\omega$ model space with the WBP interaction [18] to include the sdg major shell in the $9/2^+$ wave function (the *J*-scheme matrix dimension is about 33 000). The $g_{9/2}$ occupancy comes out to only 0.0002 in this calculation.

C. The oxygen isotope $A=22$

From the SSF measurement, we have already reported two γ rays of 3190(15) and 1380(10)keV [4] corresponding to γ decay of excited states in ^{22}O. The first one was identified to be the $2^+\rightarrow 0^+$ transition, whereas the second one was found to correspond to the decay from a higher excited state to the 2^+ state. However, no spin or parity assignment was made for this state. Recently, Thirolf *et al.* [5] have confirmed the energy and measured the electromagnetic matrix element $B(E2)$ for the 2^+ state in ^{22}O via inelastic scattering. In the DSF measurement we produced the ^{22}O nucleus by fragmentation of ^{23}F, ^{25}Ne, ^{26}Ne, ^{27}Na, and ^{28}Na. The intensity of the direct feeding of the first 2^+ level in ^{22}O has been extracted from the data corresponding to the fragmentation of different species present in the secondary beam. In the case of the one proton knock-out reactions, the intensity of the feeding of the 2^+ state in ^{22}O was found to be 19%, in good agreement with the intensity feeding (15%) given by the spectroscopic factors calculated within the USD shell model. For other reactions in which more than 2 nucleons were removed from the projectile the feeding intensity remained nearly constant with an average value of 35%.

The BaF_2 spectrum of ^{22}O, following the SSF measurement is shown in Fig. 7(a). The same spectrum obtained in the DSF experiment is shown in Fig. 7(b). One can see the improvement of the peak to background ratio obtained by the DSF method as discussed in the preceding section.

The high resolution spectrum accumulated during the SSF experiment from the Ge detectors is shown in Fig. 8. In addition to the two peaks observed in the BaF_2 spectra, one can see in this figure a previously unobserved weak γ line at 2354(6) keV. This line is more visible in the Ge spectrum where the condition that at least one BaF_2 detector signal was recorded in coincidence. This spectrum is displayed as an inset of Fig. 8. This is an indication that the 2354 keV transition is a member of a relatively long cascade in ^{22}O. This is supported by the fact that the 2354 keV transition is found to be in coincidence with the 2^+ to 0^+ 3.2 MeV transition (see Fig. 9). In addition, this figure shows two other weak γ lines. The energy of one is 3710(90), which is, within the uncertainties, equal to the sum of the 1384(4) keV and the newly observed 2354(6) keV transitions. These observations, together with the weaker intensity of the 2354 keV transition compared to that of the 1383 keV transition, strongly suggest the placement of the 2354 keV transition on the top of a γ-ray cascade as shown in the level scheme proposed in Fig. 10. We have placed the 3310 keV transition on top of the 3199 keV ground state transition. With this

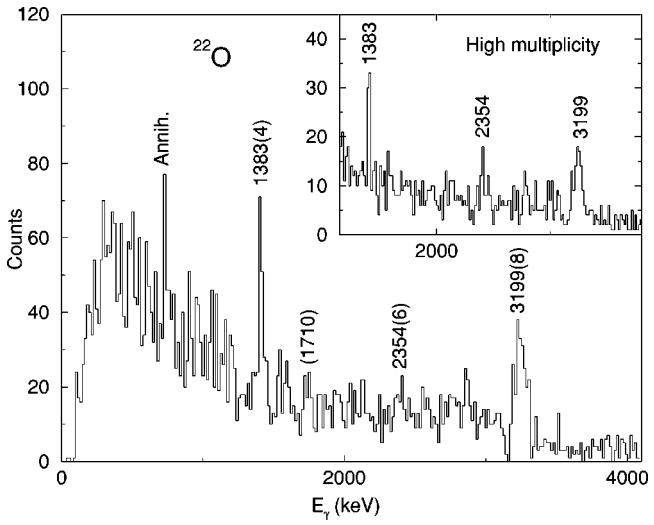

FIG. 8. High resolution γ-ray spectrum of ^{22}O obtained from the Ge detectors in the experiment using the SSF method and the same spectrum obtained by requiring a least one BaF_2 detector in coincidence (insert).

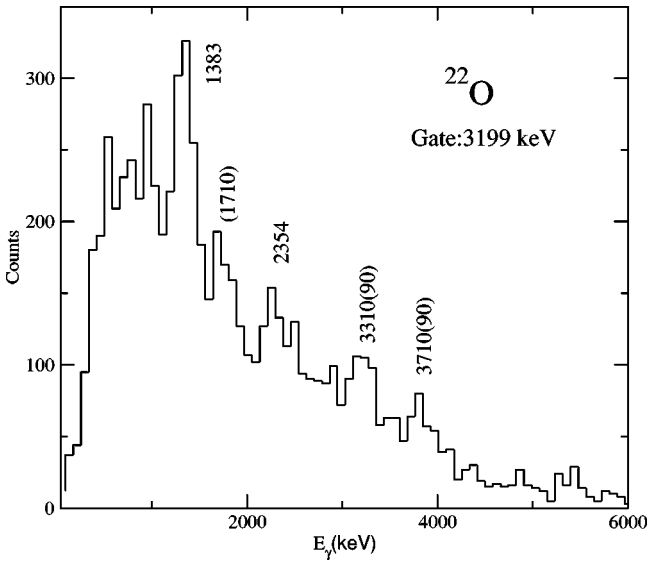

FIG. 9. BaF_2 measured γ rays observed in coincidence with the 3199 keV transition in ^{22}O during the SSF experiment.

assignment a striking agreement is obtained between the proposed level scheme for ^{22}O and the one calculated by the *sd*-shell model.

According to shell model calculations, the full *sd*-shell wave function for ^{22}O ground state is 77% $0p$-$0h$, 22% $2p$-$2h$, and 1% $4p$-$4h$ and the 2^+ energy is 3.38 MeV. Relative to the dominant $0p$-$0h$ ground state the excited states in

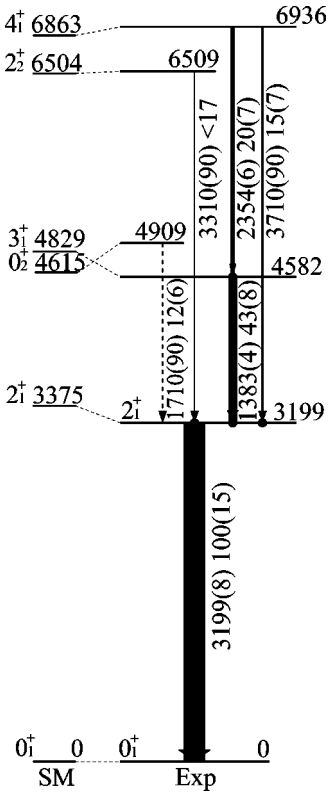

FIG. 10. The measured level scheme of ^{22}O together with the *sd*-shell-model calculations. Transition energies and relative intensities are indicated together with their uncertainties for γ lines.

^{22}O are $1p$-$1h$ with one particle in the $s_{1/2}$ or $d_{3/2}$ orbits coupled to one hole in the $d_{5/2}$ orbit. The lowest of these are the 2^+ and 3^+ states which are dominated by the $s_{1/2}$ orbit. The energies of these states are split by the residual $1p$-$1h$ interaction. Relative to the ESPE gap of 4.3 MeV the 2^+ state is pushed down to 3.4 MeV and the 3^+ state is pushed up to 4.8 MeV. The $(2J+1)$ weighted average of 4.2 MeV is close to the ESPE gap. The next states with $J=0$, 2, and 4 are those dominated by $2p-2h$ with two particles in the $s_{1/2}$ and two holes in the $d_{5/2}$. Only the lowest of these with $J=0$ is not observed in the present experiment. Although, the weak 1710 keV γ ray (seen in both Fig. 8 and Fig. 9) could account for the decay of an excited 0^+, as suggested in Fig. 10. The next levels in the calculation starting at 7.36 MeV are $1p$-$1h$ with the one particle in the $d_{3/2}$ orbital. These are well above the neutron decay threshold of 6.85(6) MeV and therefore not observed.

D. The oxygen isotope $A=23$

The information about the ^{23}O nucleus is very limited due to the experimental difficulties associated with approaching to the neutron drip line. Its S_n value is known to be 2.7(1) MeV [21]. The ground state spin and parity has been recently identified by Sauvan *et al.* [19] as $1/2^+$, in good agreement with the *sd*-shell model calculations [16].

A total number of 7500 and 19620 ^{23}O nuclei were observed in the SSF and DSF, respectively. The obtained γ-ray spectra from the BaF_2 detector array (DSF experiment) are presented in Fig. 11. Both the Doppler corrected and raw spectra exhibit relatively low statistics despite the large number of ^{23}O nuclei produced. Furthermore no clear peak is observed in the Doppler corrected spectrum. γ rays from targetlike fragments such as ^{7}Li (477 keV), ^{10}C (3353 keV), ^{11}C (2000 keV,4318 keV), ^{12}C (4439 keV), ^{10}B (718 keV, 1021 keV), ^{11}B (2124 keV,4444 keV), and ^{10}Be (3368 keV) are seen in the raw γ-ray spectrum [see Fig. 11(a)]. These are indications that there are no ^{23}O transitions with energies higher than 100 keV (the BaF_2 detector threshold).

In order to better demonstrate that the ^{23}O nucleus does not have any bound excited state, we have performed a Monte Carlo simulation of the BaF_2 array spectrum obtained from a 2.7 MeV γ ray emitted by a source moving with the velocity of the ^{23}O fragments. Since the one neutron separation energy in ^{23}O is 2.7 MeV, no γ ray is expected above this value. The lowest value of the feeding intensity of the first excited state in odd mass nuclei produced in the DSF experiment was found to be of the order of 30%. For this simulation a conservative value of 20% was taken for ^{23}O, which was experimentally populated mainly through fragmentation reactions, where many particle removal is involved. For comparison, the simulated spectrum with Doppler correction is shown in Fig. 11(b) together with that obtained from our experiment. This comparison shows convincingly that if a bound excited state existed in ^{23}O, one should clearly observe a γ peak in the measured spectrum. This remains the case even if the direct feeding intensity of this state is as low as 1%. The quality of the simulation is illustrated by the good agreement between the measured and

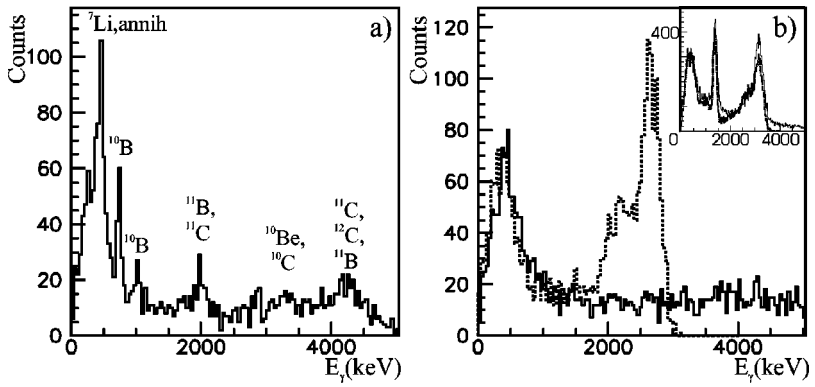

FIG. 11. (a) BaF_2 ^{23}O γ-ray spectrum without Doppler correction. The origins of the quasitarget γ emission are indicated. (b) The Doppler corrected γ-ray spectrum obtained for ^{23}O and the corresponding Monte Carlo generated spectrum (dashed line) where a 2.7 MeV simulated level deexcites (see text for details). The quality of the Monte Carlo simulation is illustrated in the inset of the figure where a comparison between the measured and simulated spectra in ^{22}O is shown. Note that the low-energy part of the simulated spectrum comes mainly from the 511 keV annihilation radiation, whereas in the measured spectrum the low-energy part is due to γ rays from various targetlike fragments (^{7}Li, ^{10}B,…). For that reason the agreement between the two spectra at low energy is purely coincidental.

calculated spectrum in the case of ^{22}O included in Fig. 11(b). The observed differences between measured and simulated spectrum are likely due to γ-ray emission from the targetlike fragments which are not taken into account in the simulation. As can be seen in the non-Doppler corrected spectrum of Fig. 11(a), these γ rays represent the major contribution in the case of ^{23}O.

For discussion we would like to note that should an excited level in ^{23}O exist, it is likely a $5/2^+$ state, which would decay to a possible $1/2^+$ ground state by an $E2$ transition. The lifetime of this state can be estimated by scaling the lifetime corresponding to the analogous 871 keV transition in ^{17}O ($t_{1/2}$=0.18 ns) to the E_γ^5 energy factor. In this case a 400 keV transition in ^{23}O would have a 8.8 ns half life, which means that most of the associated γ rays would be emitted beyond acceptance of the BaF_2 array. Hence we can propose a lower limit of about 500 keV for the energy below which the existence of a bound excited state is possible in ^{23}O. According to shell-model calculations, such a low energy for the first excited state in ^{23}O is very unlikely.

Relative to the $0p$-$0h$ model for ^{22}O, the ^{23}O levels are of $1p$-$0h$ and $2p$-$1h$ character. Of these only the lowest $1p$-$0h$ $s_{1/2}$ $(1/2^+)$ is predicted to be bound and this agrees with the present experiment. The first excited $5/2^+$ state at 2.72 MeV is the lowest state and is dominated by $2p$-$1h$ configuration. This is predicted to be very near the one-neutron decay threshold, and this experiment indicates that it lies above the neutron decay threshold.

The predicted $3/2^+$, $1p$-$0h$ state which is dominated by $d_{3/2}$ contributions lies at 3.28 MeV and is therefore also unbound to neutron decay. Such high energy for the $d_{3/2}$ orbit will mean that all of the isotopes beyond ^{24}O, where one or more nucleons resides on the $d_{3/2}$ orbit are unbound. The $d_{3/2}$ must be sufficiently unbound so that the pairing energy is not enough to bind ^{26}O (which has not been observed). According to the USD interaction in the full sd shell ^{25}O is unbound to one-neutron decay by 0.77 MeV and ^{26}O is bound to one-neutron decay by 1.77 MeV and bound to two-neutron decay by 1.00 MeV. ^{26}O would be unbound to two-neutron decay if the $d_{3/2}$ ESPE for ^{24}O would be at least 0.5 MeV higher or the pairing energy in the $d_{3/2}$ would be reduced by at least 1.0 MeV (or a combination of these).

E. The oxygen isotope $A=24$

Very little is known about this presumably heaviest bound oxygen isotope. Its lifetime and S_n value (3.7 MeV) are known with large uncertainties only. In the present experiment a relatively high yield of ^{24}O (almost 7000 nuclei) has been produced mainly by a $2p$ removal (72%) from ^{26}Ne with the remainder produced via reactions in which more than 2 nucleons were removed from the projectile. The obtained γ-ray spectra in coincidence with the ^{24}O fragments detected at the SPEG focal plane are presented in Fig. 12. Both the raw spectrum (non-Doppler corrected) and the Doppler corrected spectrum are similar to those obtained for ^{23}O. The absence of γ peaks in the Doppler corrected spectrum of ^{24}O is an indication that the first excited state in this nucleus is above the neutron decay threshold. Analogous to the ^{23}O case, a simulation has been performed and compared to the experimental result [see Fig. 12(b)]. This simulation assumes a γ transition at 3.7 MeV ($2^+ \rightarrow 0^+$) and a 2^+ feeding of 20%. Similar to the case of ^{23}O, a most conservative case has been chosen using the highest γ-ray energy possible (the neutron decay threshold in ^{24}O being 3.7 MeV [21]). The value of 20% for the feeding intensity of 2^+ in ^{24}O takes into account two contributions. One contribution comes from the nuclei produced through $2p$ removal from ^{26}Ne for which a value of 12% has been deduced using the calculated spectroscopic factors within the USD shell model. The second contribution is due to several nucleons removal fragmentation reactions; in this case a value of 35% is deduced for the feeding intensity. The comparison of the two spectra in Fig. 12(b) indicates no γ transition in ^{24}O down to a 2^+ feeding intensity of 3%.

In ^{24}O $s_{1/2}$ orbital which is relatively strongly bound in ^{23}O fills to make another magic nucleus for ^{24}O. Relative to a dominant $0p$-$0h$ wave function for the ^{24}O ground state,

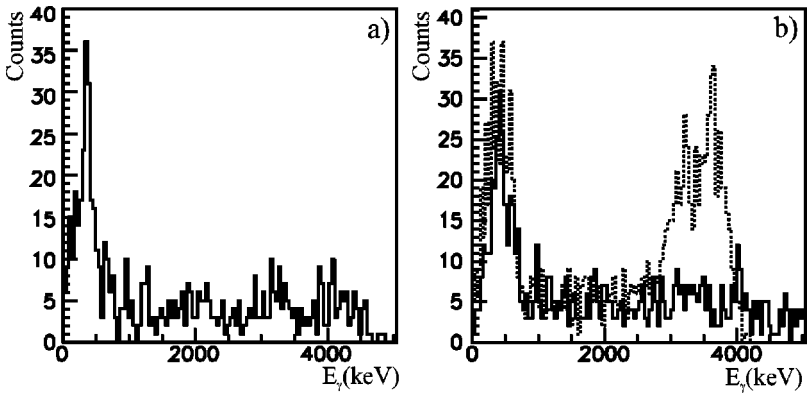

FIG. 12. (a) γ-ray spectrum of ^{24}O from the BaF_2 detectors array with no Doppler correction. (b) The Doppler corrected γ-ray spectrum obtained for ^{24}O and the corresponding Monte Carlo simulated spectrum (dashed line). In the simulation a 3.7 MeV γ ray is assumed to deexcite the first 2^+ level in ^{24}O (see text for details).

the excited states are $1p$-$1h$; $d_{3/2}$-$s_{1/2}^{-1}$ with $J=1^+$ and 2^+ and $d_{3/2}$-$d_{5/2}^{-1}$ with $J=1^+$ to 4^+. Of these the lowest is the 2^+ level predicted to be at 4.18 MeV, which is close to the neutron-decay threshold of 3.7 MeV. The nonobservation of any γ transitions in ^{24}O is consistent with theory.

IV. CONCLUSIONS AND OUTLOOK

From the study of the excited states in $^{20-24}$O through their γ decay, an estimate of the size of both $N=14$ and 16 neutron gaps could be obtained. In both cases the gaps are large and hence ^{22}O and ^{24}O are both doubly magic nuclei. The presence of the rather well bound doubly magic nucleus ^{24}O on the neutron drip line is a unique situation. These results, as well all as other properties observed for ^{20,21,22,23,24}O, are in excellent agreement with predictions made nearly 20 years ago using the USD effective Hamiltonian. The $T=1$ part of the USD Hamiltonian, which is responsible for this behavior is essentially different from that predicted from the renormalized G matrix and the reason for the difference is not understood.

It appears that while the $N=16$ shell gap turns out to be larger than 3 MeV in the heaviest oxygen isotopes, it is only of the order of 1 MeV in the silicon and magnesium isotopes. This can be accounted for by considering the role of the strong n-p monopole interaction acting between the two spin-orbit partners $\pi d_{5/2}$ and $\nu d_{3/2}$ [22]. As the $d_{5/2}$ proton orbital is emptied this interaction is released and the $d_{3/2}$ neutron orbital is shifted towards the fp shell decreasing in the same time the $N=20$ shell gap and increasing the $N=16$ gap. This evolution of the neutron $d_{3/2}$ orbital is complete in the Oxygen isotopes where the $\pi d_{5/2}$ is empty, making the $N=16$ shell gap relatively larger. Such a large $N=16$ gap in oxygen isotopes is probably the reason why heavier isotopes having $N=18$ and 20 are neutron unbound (as the $\nu d_{3/2}$ lies at higher energy than in Mg and Si nuclei).

Further studies should be performed to detect the neutron decay of the particle-unbound states of ^{23,24}O or by using transfer reactions in order to firmly establish the energy of the first excited states in these nuclei and consequently determine the size of the $N=16$ gap in oxygen. The determination of the size of the $N=16$ gap in F and Ne is also important in order to complete the study of the single-particle evolution and its effect on the drip-line location in this region.

ACKNOWLEDGMENTS

The experiment using in-beam γ-ray spectroscopy following projectile fragmentation benefited from the smooth operation of the accelerator by the GANIL operations team. The use of segmented clover detectors was made possible by the EXOGAM Collaboration. This work was supported by the European Community Contract No. HPRI-CT-1999-00019, and also from OTKA-D34587, T38404, T42733, PICS(IN2P3) 1171, INTAS 00-0043 and RFBR N96-02-17381a grants, as well as from Bolyai Janos Foundation. B.A.B. acknowledges support from NSF grant (Grant No. PHY-0244453).

[1] O. Tarasov *et al.*, Phys. Lett. B **409**, 64 (1997).
[2] H. Sakurai *et al.*, Phys. Lett. B **448**, 180 (1999).
[3] W. N. Catford *et al.*, Nucl. Phys. **A503**, 263 (1989).
[4] M. Belleguic *et al.*, Nucl. Phys. **A682**, 136c (2001).
[5] P. G. Thirolf *et al.*, Phys. Lett. B **485**, 16 (2000).
[6] A. Ozawa *et al.*, Phys. Rev. Lett. **84**, 5493 (2000).
[7] Z. Dlouhy *et al.*, *International Nuclear Physics Conference*, edited by Eric Norman, Lee Schroeder, and Gordon Wozniak, AIP Conf. Proc. No. 610 (AIP, Melville, NY, 2002), p. 736.
[8] Ozawa *et al.*, Nucl. Phys. **A691**, 559 (2001).
[9] B. A. Brown, P. G. Hansen, and J. A. Tostevin, Phys. Rev. Lett. **90**, 159201 (2003).
[10] R. Kanungo *et al.*, Phys. Rev. Lett. **88**, 142502 (2002).
[11] K. Yoneda *et al.*, Phys. Lett. B **499**, 233 (2001).
[12] B. H. Wildenthal, Prog. Part. Nucl. Phys. **11**, 5 (1984).
[13] B. A. Brown and B. H. Wildenthal, Annu. Rev. Nucl. Part. Sci. **38**, 29 (1988).
[14] T. T. S. Kuo and G. E. Brown, Nucl. Phys. **85**, 40 (1966); T. T. S. Kuo, Nucl. Phys. **A103**, 71 (1967).
[15] S. LaFrance *et al.*, Phys. Rev. C **20**, 1673 (1979).

[16] B. A. Brown, http://www.nscl.msu.edu/~brown/decay/
[17] B. A. Brown, Prog. Part. Nucl. Phys. **47**, 517 (2001).
[18] E. K. Warburton and B. A. Brown, Phys. Rev. C **46**, 923 (1992).
[19] E. Sauvan *et al.*, Phys. Lett. B **491**, 1 (2000).
[20] B. A. Brown, Prog. Theor. Phys. Suppl. **146**, 23 (2002).
[21] G. Audi and A. H. Wapstra, Nucl. Phys. **A595**, 409 (1995).
[22] T. Otsuka *et al.*, Phys. Rev. Lett. **87**, 082502 (2001).